Physicochem. Probl. Miner. Process., 61(4), 2025, 208077

http://www.journalssystem.com/ppmp

Physicochemical Problems of Mineral Processing

ISSN 1643-1049

Efficient separation of K-feldspar and fluorapatite using decyldimethylammonium chloride as a novel collector

Zining Guo, Haoran Sun, Yulian Wang, Gui Gao

School of Materials Science and Engineering, Shenyang Ligong University, Shenyang 110159, China

Corresponding author: 18842504743@163.com (Haoran Sun)

Abstract: Selective modulation of the surface properties of K-feldspar and fluorapatite is the key to achieving efficient separation of the two. In this study, Decyldimethylammonium Chloride (DDAC) was used as a novel collector to achieve flotation separation of K-feldspar and fluorapatite. The results of flotation experiments showed that K-feldspar could be selectively floated when the concentration of DDAC was 10 mg/L at pH=3.0, and the recovery of K-feldspar reached 97.07%, while the recovery of fluorapatite was only 6.68%. Zeta potential test proved that the cationic collector DDAC could selectively increase the surface potential of K-feldspar, and the increase of K-feldspar potential at DDAC concentration of 30mg/L was 43.5 times that of fluorapatite. Infrared spectroscopy and XPS detection revealed that DDAC selectively reacted with oxygen sites on the surface of K-feldspar and adsorbed on the surface of K-feldspar through hydrogen bonding and electrostatic adsorption, but had no effect on fluorapatite.

Keywords: K-feldspar, fluorapatite, DDAC, flotation, selective adsorption

1. Introduction

Fluorapatite ($Ca_5(PO_4)_3F$) is an important phosphorus-containing mineral resource that plays a central role in the phosphorus fertilizer and phosphorus chemical industries. As the primary raw material for global agricultural phosphorus fertilizer production, it is crucial for promoting plant growth and enhancing soil fertility (Hogen et al., 2024; Liu et al., 2025). Geological exploration data indicates that over 70% of the identified fluorapatite ore deposits worldwide exhibit the coexistence of fluorapatite and K-feldspar (K_2O-Al_2O_3-$6SiO_2$) (Miao et al., 2024). K-feldspar is a key raw material for the glass and ceramics industries (García-ten et al., 2024; Xu et al., 2025;). In actual mining operations, the two minerals often coexist as a composite ore. For example, in some mining areas in China, each 100 tons of raw ore contains approximately 30–50 tons of fluorapatite and 20–40 tons of K-feldspar. Due to their similar surface properties (Liu et al., 2024), separating them is challenging, and failure to do so severely impacts product quality—residual K-feldspar in phosphate fertilizers reduces fertilizer efficacy, while fluorapatite contamination in glass raw materials leads to decreased product strength. Therefore, achieving efficient separation of the two is crucial for enhancing resource utilization and ensuring industrial product quality.

In the flotation separation of K-feldspar and fluorapatite, relevant scholars have conducted research on this topic. Chao et al. (2018) investigated the effect of $BaCl_2$ on K-feldspar flotation under natural pH conditions using DDAC as the collector. The results showed that low $BaCl_2$ concentrations enhanced K-feldspar floatability, while high concentrations significantly inhibited it. Larsen et al. (2019) developed a selective flotation process to separate K-feldspar from albite. K-feldspar flotation was conducted in an alkaline environment (pH 10.5–11.6) using NaOH as the modifier and nonionic Brij58 as the frother. The flotation produced a K-feldspar concentrate with 14.3% K_2O, 77% recovery, and a K_2O/Na_2O ratio of 10.4. Yi et al. (2023) investigated the effects and mechanisms of Al(III) and Fe(III) ions on K-feldspar flotation efficiency in oleate collector systems. Al(III) and Fe(III) ions significantly improved K-feldspar flotation recovery by modifying its surface charge, bonding properties, and adsorption behavior. Due to the high cost and complexity of existing flotation techniques, developing a selective collector for K-

DOI: 10.37190/ppmp/208077

feldspar is essential. This will improve flotation efficiency by introducing a cost-effective and environmentally friendly collector.

DDAC is a typical quaternary ammonium salt-based cationic surfactant that combines high surface activity with antimicrobial properties（Nowicka-Krawczyk et al., 2015; Hafidi et al., 2025）. Its molecular structure comprises a long-chain alkyl hydrophobic end and a quaternary ammonium salt hydrophilic end, conferring excellent interfacial adsorption capacity and water solubility. The molecular structure of DDAC is illustrated in Fig. 1. It remains chemically stable under acidic to weakly alkaline conditions and can strongly bind to negatively charged mineral surfaces or microbial cell membranes via electrostatic interactions (Jiang et al., 2024). It is commonly used industrially as a broad-spectrum antimicrobial agent, widely applied in water treatment, food processing, and healthcare fields, capable of rapidly inactivating bacteria, fungi, and other microorganisms at low concentrations (Zhang et al., 2025). In summary, DDAC, due to its low bioaccumulation, good degradability, and strong adsorption properties toward minerals, can serve as a potential collector in the mineral processing field.

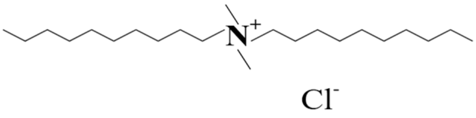

Fig. 1 Molecular structure of DDAC

In this study, we first evaluated the effect of DDAC on mineral separation through flotation experiment. Subsequently, we employed zeta potential measurements, Fourier transform infrared spectroscopy (FTIR), and X-ray photoelectron spectroscopy (XPS) to investigate the interaction mechanisms between DDAC and the minerals.

2. Test materials and methods

2.1. Test material

The K-feldspar samples used in this experiment were sourced from the Haicheng area of Liaoning, while the fluorapatite samples were obtained from the Dashiqiao area of Liaoning. The lump ore was manually selected, crushed, and subjected to vibratory screening to ensure a homogeneous mixture of powders. Finally, ore samples with a particle size between -74 +44 μm were prepared for subsequent experimental studies. The prepared K-feldspar and fluorapatite samples underwent chemical multi-element analysis and X-ray diffraction analysis. The results of the X-ray diffraction analysis are shown in Fig. 2, and the results of the chemical multi-element analysis are presented in Table 1. According to the test results, the purity of fluorapatite and K-feldspar reached 99.5% and 95%, respectively, meeting the standards required for single-mineral flotation experiment. The chemically pure reagent DDAC used in this study was provided by Shanghai MacLean Biochemical Technology Co., Ltd. During the flotation experiment, deionized water was used throughout to ensure consistent water quality. Additionally, hydrochloric acid and sodium hydroxide were employed as pH adjusters to maintain pH stability during the experiment.

Table 1. Multi-element analysis of single mineral chemistry

Sample	Al_2O_3	SiO_2	Fe_2O_3	CaO	MgO	K_2O	Na_2O	TiO_2	Purity
K-feldspar	16.95	66.62	0.19	0.09	0.06	15.01	0.56	0.03	95.02
Fluorapatite	-	0.08	0.09	52.86	0.03	0.01	0.09	-	99.55

2.2. Flotation experiment

In the single-mineral and binary mixed ore flotation experiments of K-feldspar and fluorapatite, 2 g of ore sample was chosen for each experiment. The experiment was carried out using a hanging tank flotation machine with a capacity of 30 ml. The slurry was agitated for 2 minutes at the start of the experiment, followed by pH adjustment and collector addition in the order specified by the flotation experiment procedure. The froth scraping process lasted for 3 minutes, and the flotation machine's rotational speed was set to 1800 rpm, with 20 ml of deionized water added. After the experiment, each concentrate was dried and weighed. The flotation experiment flow is shown in Fig. 3.

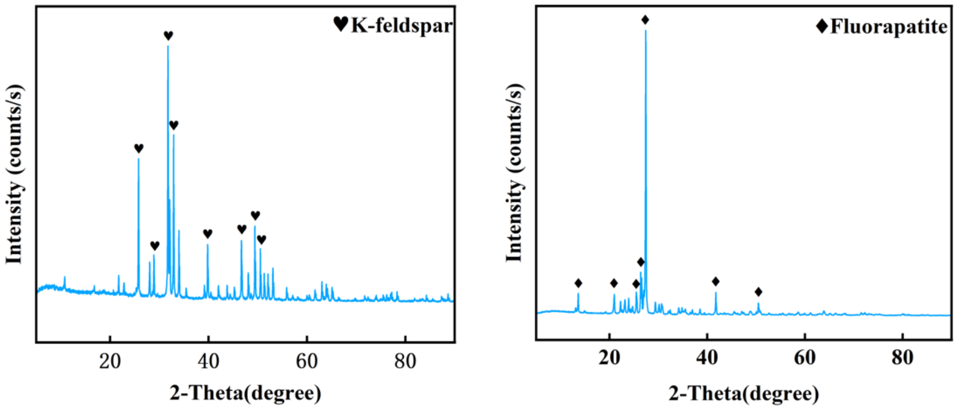

Fig. 2. The XRD analysis of mineral samples

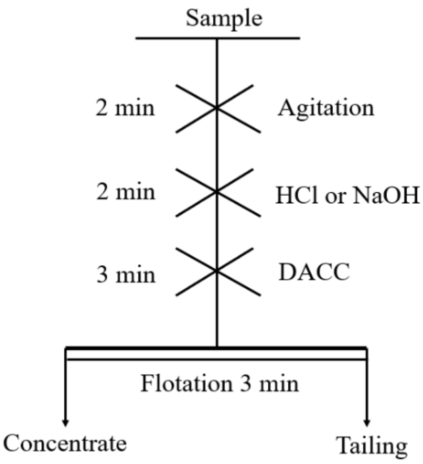

Fig. 3. Flotation experiment flow

2.3. Zeta potential test

The zeta potential of mineral particles was measured using a Malvern Zetasizer Nano ZS instrument (Malvern, UK) to evaluate the impact of DDAC on the surface electrical properties of fluorapatite and K-feldspar. Before the experiments, the mineral samples were ultrasonically dispersed to prevent particle aggregation. The mineral suspensions were prepared as slurries with a solid-to-liquid ratio of 1:100, and the pH was adjusted to 3.0 to ensure stability. The changes in zeta potential on the mineral surfaces were measured at different DDAC concentrations, with at least three replicate measurements taken at each pH condition and averaged. The influence of DDAC on surface charge modification was investigated using the electrophoretic light scattering (ELS) technique.

2.4. FTIR testing

FTIR analysis was conducted using a Nicolet iS50 spectrometer (Thermo Fisher, USA) to examine the interaction between DDAC and surface functional groups of minerals. Before analysis, fluorapatite and K-feldspar samples were dried at 105°C for 4 hours to eliminate surface moisture. The dried samples were thoroughly mixed and ground with KBr at a 1:100 mass ratio, then pressed into 13 mm diameter translucent pellets. FTIR spectra were acquired over a wavelength range of 4000-400 cm^{-1} with a resolution of 4 cm^{-1}, and 32 scans were accumulated for each sample to enhance the signal-to-noise ratio. The adsorption mechanism of DDAC on fluorapatite and K-feldspar surfaces was elucidated through systematic analysis of adsorption peak variations by comparing IR spectra before and after DDAC treatment.

2.5. XPS analysis

Thermo Scientific's VG ESCALAB 250Xi spectrometer was used to collect XPS spectra of samples before and after treatment with flotation chemicals at precise pH values. To assure data accuracy, the C1s peak at 284.80 eV was used as the internal binding energy scale for calibration. First, 2 g of the sample was added to 20 mL of deionized water and processed using the preset flotation test protocol. After treatment, the solid-liquid separation was achieved by centrifugation at 3000 rpm for 10 minutes. The solid minerals were rinsed three times with deionized water and dried at 313K. The solid minerals were then dried at a temperature of 277.65K (4.5 degrees Celsius). Finally, the dried solid minerals were analyzed using XPS spectroscopy.

3. Experimental results

3.1. Single mineral floatability experiment

3.1.1 Effect of amine concentration on the flotation performance of single minerals

Fig. 4 shows the differential study of dodecyl amine (DDA) and octadecyl amine (ODA) concentrations on the flotation of K-feldspar and fluorapatite.

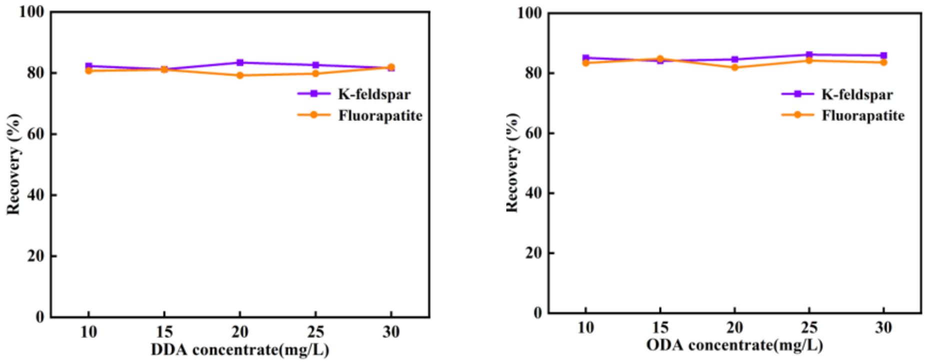

(a) DDA (b) ODA

Fig. 4. The effect of DDA and ODA concentrations on the flotation performance of K-feldspar and fluorapatite

Fig. 4 demonstrates that when DDA and ODA are used as collectors, the flotation recovery of fluorapatite and K-feldspar remain within the range of 80−85% across the tested concentration gradient, with a recovery difference of less than 5% between the two minerals. This result indicates that traditional amine-based collectors fail to achieve effective separation of the two minerals, thereby highlighting the critical necessity of employing DDAC as a novel collector in this study.

3.1.2. Effect of pH on the floatability of single minerals

The concentration of DDAC was set at 30 mg/L, and the effect of pulp pH on the floatability of K-feldspar and fluorapatite was investigated, the findings are given in Fig. 5.

As depicted in Fig. 5, DDAC demonstrates excellent collecting performance for K-feldspar across various pH conditions, maintaining a stable recovery of approximately 96%. However, the recovery of fluorapatite exhibits significant variations with changes in pH: within the pH range of 3.0 to 7.0, the recovery of fluorapatite increases significantly from 6.68% to 70.42%. When the pH value further increases from 7.0 to 11.0, the recovery gradually decreases to 38.04%. Comparative analysis reveals that the largest difference in recovery between K-feldspar and fluorapatite occurs at pH 3.0, reaching 89.32%. Therefore, pH 3.0 is determined as the optimal pH condition for the flotation separation of the two minerals.

3.1.3. Effect of DDAC concentration on the floatability of single minerals

The effect of DDAC concentration on the floatability of K-feldspar and fluorapatite was investigated at pH=3.0, and the experiment results are shown in Fig. 6.

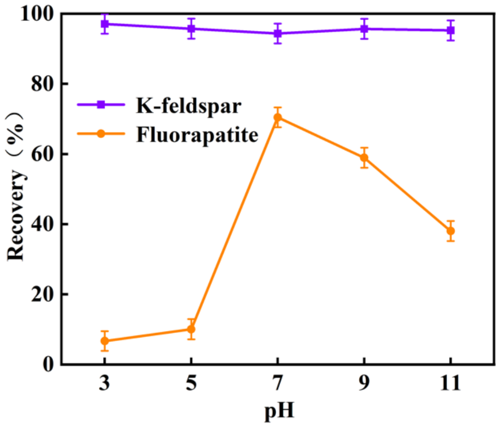

Fig. 5. Effect of pH on the floatability of K-feldspar and fluorapatite

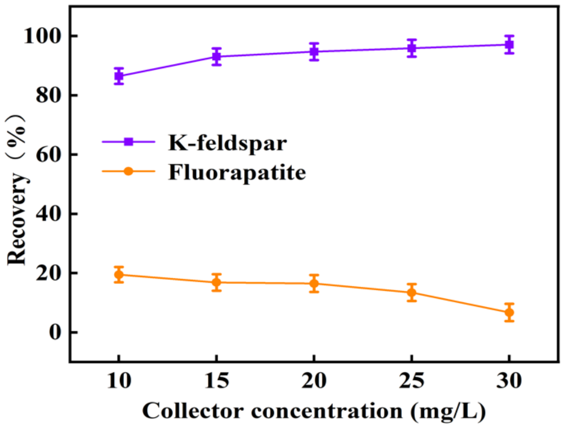

Fig. 6. Effect of DDAC concentration on the floatability of K-feldspar and fluorapatite

As shown in Fig. 6, when the concentration of DDAC is 10 mg/L, the recovery of K-feldspar is 86.45%. When the concentration of DDAC increases to 30 mg/L, the recovery of K-feldspar significantly rises to 97.07%. Conversely, the recovery of fluorapatite exhibits a decreasing trend with the increase in DDAC concentration. Specifically, when the concentration of DDAC is 10 mg/L, the recovery of fluorapatite stands at 19.45%. However, when the concentration of DDAC increases to 30 mg/L, its recovery drops significantly to 6.68%. Therefore, under the conditions of a DDAC concentration of 30 mg/L and a pulp pH of 3.0, the separation effect between K-feldspar (97.07%) and fluorapatite (6.68%) is more pronounced.

3.2. Artificial mixed ore flotation separation experiment

To further enhance the flotation separation of fluorapatite and K-feldspar under different conditions, an artificial mixed ore flotation separation experiment was conducted following the flotation experiment process shown in Fig. 2. Table 2 shows an artificial mixed ore flotation experiment using a total of 2.0 grams of minerals, with the mixed ore ratios of fluorapatite to potassium feldspar set at 7:3 and 1:1.

Table 2. Artificial mixed ore experiment results

Mixed ore ratio	Sample	Productivity/%	Grade /%		Recovery /%	
			P_2O_5	Al_2O_3	Fluorapatite	K-feldspar
Fluorapatite : K-feldspar =1:1	concentrate	43.89	69.12	0.96	82.81	4.97
	ore	100.00	21.93	8.47	100.00	100.00
Fluorapatite : K-feldspar =7:3	concentrate	60.77	67.82	1.71	78.05	20.43
	ore	100.00	30.702	5.08	100.00	100.00

As indicated in Table 2, under a 1:1 ratio, the grade of P_2O_5 in the concentrate is 69.12%, the recovery of fluorapatite is 82.81%, and the recovery of K-feldspar is merely 4.97%. When the ratio is adjusted to 7:3, the grade of P_2O_5 in the concentrate drops to 67.82%, the recovery of fluorapatite increases to 78.05%, and the recovery of K-feldspar climbs to 20.43%. These findings reveal that, despite an upward trend in the recovery of K-feldspar, DDAC still favors the flotation of fluorapatite. This verifies DDAC's potential as an efficient collector for the selective separation of fluorapatite and K-feldspar.

3.3. Mechanism of action analysis

3.3.1. Zeta potential results

The interaction of flotation agents with mineral surfaces modifies their surface properties, consequently affecting the flotation behavior of mineral particles (Yao, 2024). Zeta potential analysis has been extensively employed in mineral flotation separation studies to investigate surface-agent interactions (Han et al., 2021; Luo et al., 2024; Teng et al., 2018). Fig. 7 presents the zeta potential measurement results demonstrating the surface charge variations of fluorapatite and K-feldspar before and after exposure to flotation reagents.

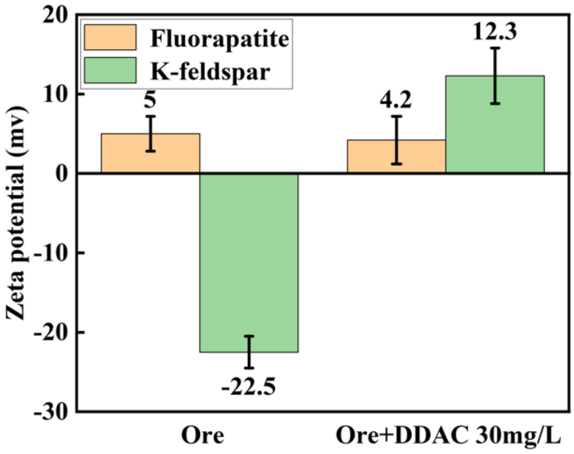

Fig. 7. Zeta potential of mineral surfaces before and after DDAC at pH=3.0

As illustrated in Fig. 7, the Zeta potential test conducted under pH 3.0 conditions revealed that in the absence of DDAC, the surface of fluorapatite exhibited a weak positive Zeta potential (+5.0 mV), whereas the surface of K-feldspar displayed a strong negative Zeta potential (-22.5 mV). Upon the addition of DDAC, the Zeta potential of fluorapatite slightly decreased to +4.2 mV. Conversely, due to electrostatic attraction, positively charged DDAC tends to adsorb onto the negatively charged surface of K-feldspar, leading to a significant positive shift in the Zeta potential of K-feldspar, reaching +12.3 mV. The surface potential of fluorapatite underwent only minor changes, indicating that DDAC primarily adsorbed onto the surface of K-feldspar, with only a small amount adsorbed onto the surface of fluorapatite. These results suggest that the synergistic effect of hydrogen bonding and electrostatic adsorption facilitates the strong adsorption of DDAC on the surface of K-feldspar, thereby achieving efficient separation between K-feldspar and fluorapatite.

3.3.2. FTIR results

Infrared spectroscopy serves an effective analytical tool for characterizing surface functional groups of materials (Payerl et al., 2017; Tian et al., 2022; Cheng et al., 2024). By detecting infrared absorption peaks, the vibrational modes of chemical bonds within molecules can be identified, thereby revealing the interaction mechanisms between minerals and collectors (Wang et al., 2022). Since different chemical bonds or functional groups exhibit characteristic absorption peaks within specific wavelength ranges, this study systematically analyzed the chemical structural changes on the surfaces of fluorapatite and K-feldspar before and after DDAC treatment using FTIR spectroscopy, aiming to investigate their adsorption mechanisms (Fig. 8).

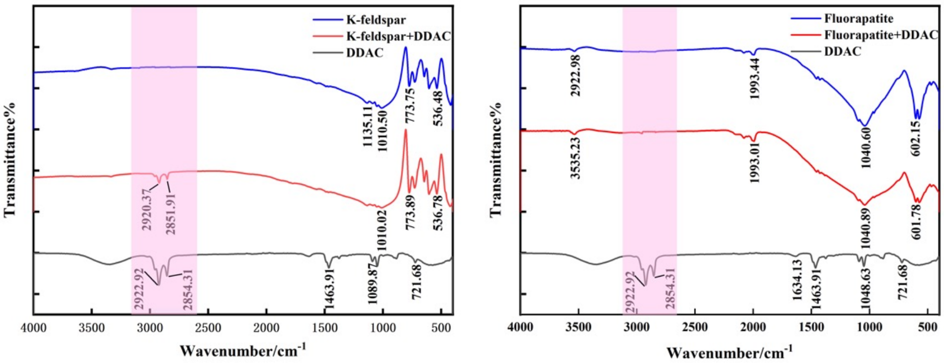

Fig. 8. Infrared spectra of K-feldspar and fluorapatite before and after DDAC action

As summarized in Fig. 8, the main absorption peak of the infrared spectrum of fluorapatite remained essentially unchanged before and after the addition of DDAC. Specifically, the characteristic absorption peaks at 1093.01 cm^{-1}, 1040.89 cm^{-1}, 601.7 cm^{-1}, and 572.15 cm^{-1} exhibited only minor shifts, with no significant changes observed. In contrast, K-feldspar exhibited pronounced spectral changes after DDAC treatment: two new absorption peaks emerged at 2920.37 cm^{-1} and 2851.91 cm^{-1}, corresponding to the symmetric and asymmetric stretching vibrations of the C-H bonds in the DDAC alkyl chain, respectively. Simultaneously, the main absorption peaks of K-feldspar at 1010.02 cm^{-1}, 772.9 cm^{-1}, and 536.76 cm^{-1} shifted significantly. The comparative analysis of infrared spectra revealed that the interface interaction between K-feldspar and DDAC was significantly stronger than that in the fluorapatite-DDAC system, further confirming DDAC's high selective adsorption capacity for K-feldspar.

3.3.3. XPS results

XPS is a highly efficient characterization technique that can be used to analyze the elemental composition, chemical state, molecular structure, and surface content of material surfaces (Liu , 2024; Moeini et al., 2023; Hu et al., 2024). In this study, the adsorption behavior of DDAC on the surface of fluorapatite and K-feldspar was analyzed by XPS (Figs. 9 and 10), focusing on the full spectra of the minerals before and after the treatment of DDAC, the changes in the elemental composition of the surfaces, the binding energies, and their interactions with the oxygen centers (Figs. 11 and 12), thus revealing the mechanism of the selective adsorption of DDAC on the surface of K-feldspar.

As shown in Fig. 9, the surface of K-feldspar without DDAC treatment primarily exhibited characteristic peaks of K2p, Si2p, Al2p, O1s, and C1s. After DDAC treatment, a distinct N1s peak emerged in the XPS spectrum, originating from the nitrogen element in the quaternary ammonium salt ion $[(C_{10}H_{21})_2N(CH_3)]^+$ present in DDAC, thus indicating successful adsorption of DDAC on the K-feldspar surface. Conversely, the chemical composition of fluorapatite remained largely unchanged before and after DDAC treatment. Its XPS spectra predominantly displayed characteristic peaks such as Ca2p, P2p, O1s, and C1s, suggesting a weaker adsorption capacity of DDAC on the fluorapatite surface.

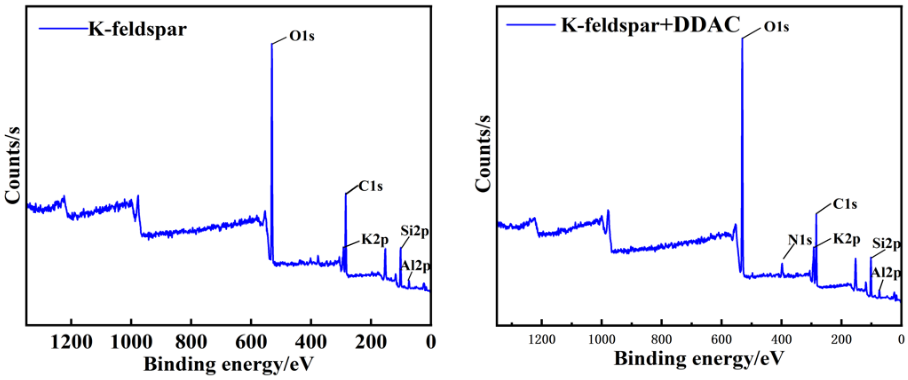

Fig. 9. Mineral X-ray photoelectron full spectrum of K-feldspar before and after DDAC action

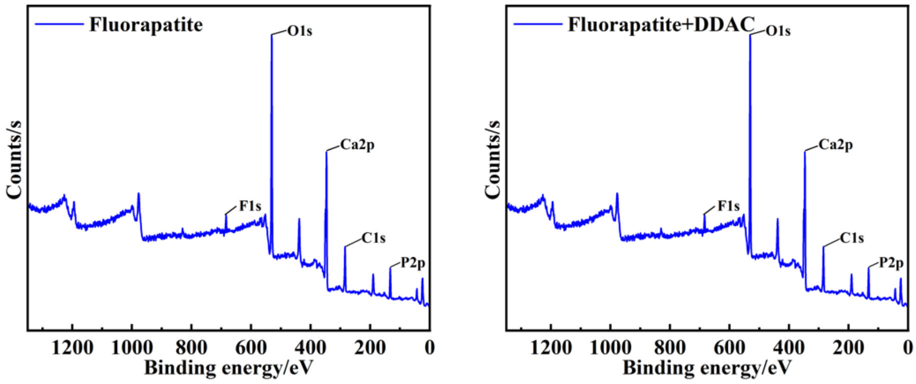

Fig. 10. Mineral X-ray photoelectron full spectrum of fluorapatite before and after DDAC action

Table 3 presents the variations in surface elemental composition of K-feldspar and fluorapatite before and after DDAC treatment. Following treatment, the N1s concentration on the K-feldspar surface increased to 0.81%, and the C1s content rose significantly from 26.10% to 40.46%. This increase aligns with the adsorption behavior of the DDAC alkyl chain, indicating substantial adsorption of DDAC on the K-feldspar surface. Concurrently, the decrease in O1s content likely results from the surface being coated by organic molecules, thereby reducing oxygen exposure. In contrast, fluorapatite exhibited minimal changes in surface composition post-DDAC treatment: the C1s concentration saw a slight increase from 30.12% to 30.27%, no N1s signal was detected, and the O1s concentration remained largely unchanged. These findings further corroborate the weak interaction between DDAC and fluorapatite.

Table 3. Comparison of binding energy and mineral surface element composition before to and following DDAC activity

Sample	Elemental content % (Binding energy /eV)					
	K2p	Si2p	Al2p	C1s	O1s	N1s
K-feldspar	4.82 (293.15)	17.7 (102.05)	6.43 (73.75)	26.10 (284.80)	44.94 (531.23)	0
K-feldspar +DDAC	2.59 (292.42)	15.65 (101.36)	5.04 (73.19)	40.46 (284.80)	35.04 (530.83)	0.81 (399.87)
Fluorapatite	0	2.78 (100.74)	0	30.12 (284.80)	51.20 (530.79)	0
Fluorapatite +DDAC	0	2.73 (100.62)	0	30.27 (284.80)	51.08 (530.80)	0

The O1s binding energy of fluorapatite and K-feldspar was analyzed, as shown in Figs. 11 and 12. The results indicate that the O1s binding energy of K-feldspar significantly decreased from 531.23 eV to 530.83 eV after DDAC treatment, suggesting a strong interaction between the cationic quaternary ammonium group of DDAC and the oxygen centers on the K-feldspar surface, which altered the chemical environment of the oxygen atoms. In contrast, the O1s binding energy of fluorapatite remained nearly unchanged before (530.79 eV) and after treatment (530.80 eV), demonstrating negligible interaction between DDAC and the oxygen sites on the fluorapatite surface, and thus minimal surface adsorption. These findings are consistent with the XPS full-spectrum data and elemental composition analysis, further confirming the weak adsorption capacity of DDAC on the fluorapatite surface.

3.4. Modeling the separation of K-feldspar and fluorapatite

Based on experimental and mechanistic, the modeling of the separation of K-feldspar and fluorapatite in the presence of a DDAC collector is shown in Fig. 13.

DDAC is a double-chain quaternary ammonium salt cationic surfactant. In solution, DDAC exists as $[(C_{10}H_{21})_2N(CH_3)]^{2+}$. Under acidic conditions, the Si-O functional groups on the K-feldspar surface acquire a negative charge, enhancing their ability to adsorb cations. In contrast, the PO_4^{3-} groups in

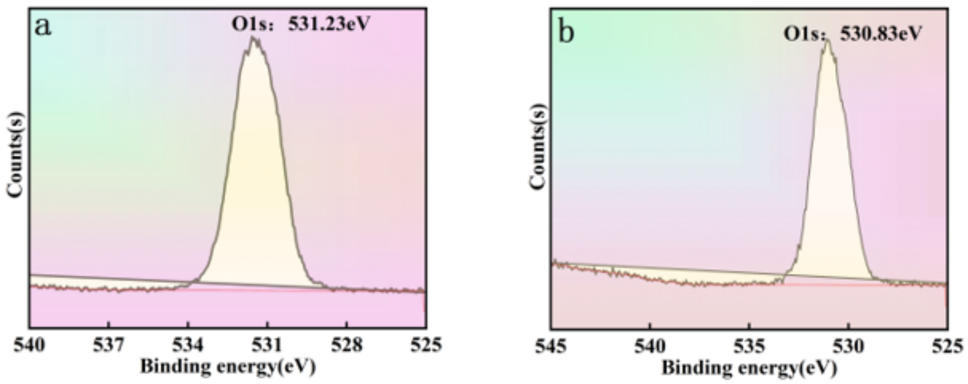

Fig. 11. Binding energy of O on K-feldspar before (a) and after (b) DDAC treatment

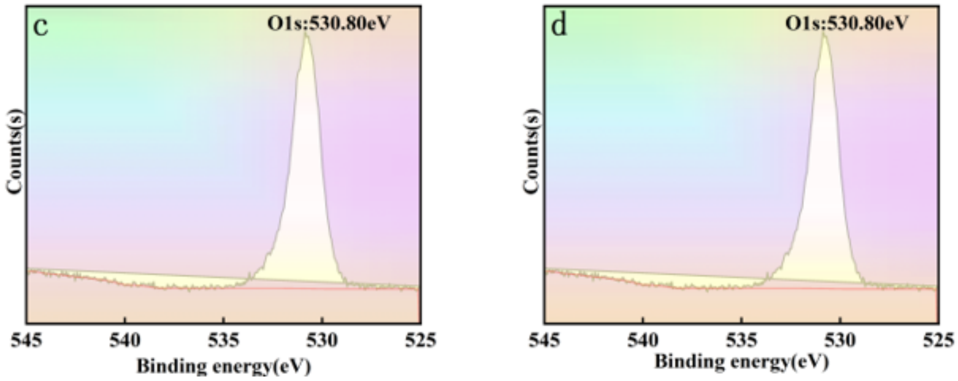

Fig. 12. Binding energy of O on fluorapatite before (c) and after (d) DDAC treatment

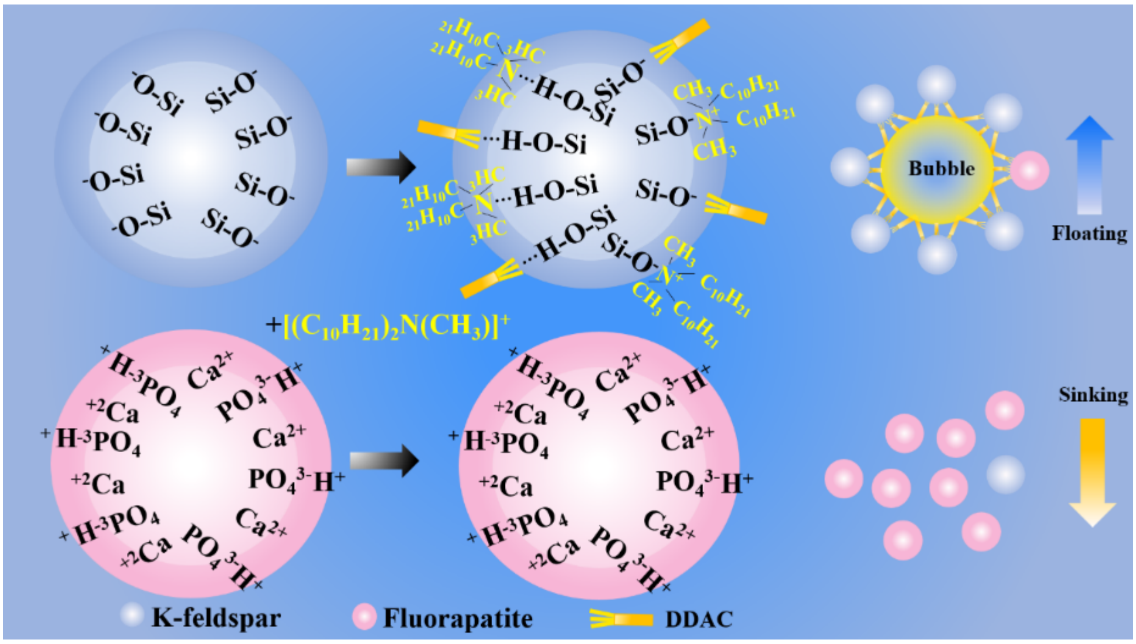

Fig. 13. Modeling the separation of K-feldspar and fluorapatite in the presence of DDAC collector

fluorapatite undergo protonation upon interaction with H^+ ions, leading to the release of Ca^{2+} and disruption of the surface charge balance, resulting in a net positive charge on the fluorapatite surface. The positively charged DDAC selectively adsorbs onto the K-feldspar surface through hydrogen bonding and electrostatic interactions, with its hydrophobic groups rendering the mineral surface hydrophobic and promoting bubble attachment, thereby facilitating flotation. Conversely, fluorapatite, due to its strong hydrophilicity and minimal DDAC adsorption, sinks, enabling the effective separation of the two minerals (Liu et al., 2017; Yao et al., 2025; Gao et al., 2024).

4. Conclusions

This systematic investigation elucidates the selective mechanism of DDAC as a collector for separating fluorapatite from K-feldspar, yielding three principal findings:

1. Maximum differentiation in recovery (K-feldspar vs. fluorapatite) reached 82.6% under optimal conditions (pH 3.0, 30 mg/L DDAC concentration), demonstrating DDAC's preferential affinity for K-feldspar.
2. Surface potential analysis revealed a charge reversal on K-feldspar (from negative to positive) through DDAC adsorption, mediated by combined electrostatic interactions and hydrogen bonding. FTIR spectroscopy confirmed these interfacial interactions, while fluorapatite exhibited negligible response under identical conditions.
3. XPS analysis identified specific oxygen site interactions on K-feldspar surfaces, providing electronic structure evidence for DDAC's selective adsorption behavior. No comparable binding sites were detected on fluorapatite.

Acknowledgments

This work was financially supported by National Natural Science Foundation of China (No. 52404290 & 52374271). The research was also funded by The Basic Research Projects in Higher Education Institutions of the Department of Education of Liaoning Province (LJ212410144037).

References

HOGEN, T., BARBANA, N., KEMPER, S., BECKER, J. , AL-ADDOUS, J., AL-ADDOUS, M., GEISSEN, S., 2024. *A contribution to the development of a process to valorize the wastewater of wet phosphate fertilizer production*. J Environ Chem Eng. 12(5), 113699.

LIU, R., DENG, L., CHU, J., XU,W., ZHOU, G., ZHANG, Y., HE, j., LI, G., CAO, Y., 2025. *Flotation separation mechanisms of fluorapatite and muscovite by fatty acid and polyoxymethylene ether phosphate in hard water.* Sep Purif TechnoL. 360,131126.

GARCÍA-TEN, J., DONDI, M., VIEIRA LISBOA, J., CABEDO, M., PÉREZ-VILLAREJO, L., RAMBALDI, E., ZANELLI , C., 2024. *Critical raw materials in the global high-throughput ceramic industry*. Sustain Mater Techno. 39, e00832.

XU. H., SUN, Q., SUN, W., HAN, X., ZHANG, K., 2025. *Preparation and sintering mechanism of foamed ceramics from iron tailings and feldspar powder*. Ceram Int. 51(17), 24123-24135.

MIAO, Z., XU, B., HOU, Q., ZHAO, Z., 2024. *Identifying recycled oceanic components and volatiles in the Lizhuang carbonatite-associated REE deposit in southwest China: New constrain from in situ Hf–O isotopes*. Ore Geol Rev. 165, 105872.

LIU, C., HE, H., ZHU, Y., XU, W., YANG, S., 2024. *The utilization of 1-Dodecyl-3-methylimidazolium bromine ionic liquid in the reverse flotation separation of feldspar from apatite.* Adv Powder Technol. 35(6),104499.

SONG, C., ZHOU, Y., LIU, Q., DENG, J., LI, S., GAO, L., YU, L., 2018. *Effects of $BaCl_2$ on K-feldspar flotation using dodecyl amine chloride under natural pH*. T Nonferr Metal Soc. 28(11), 2335-2341.

LARSEN, E., JOHANNESSEN, N., B. KOWALCZUK, P., KLEIV, R., 2019. *Selective flotation of K-feldspar from Na-feldspar in alkaline environment.* Miner Eng. 142, 105928.

YI, C., ZHOU, J., HE, G., HU, H., LIU, C., YANG, J., LYU, X., 2023. *The effect of Al(III) and Fe(III) ions on the flotation behavior of k-feldspar with sodium oleate as the collector.* Physicochem Probl Mi. 59(6), 1747124.

NOWICKA-KRAWCZYK, P., ŻELAZNA-WIECZOREK, J., KOZIRÓG, A., OTLEWSKA, A., RAJKOWSKA, K., PIOTROWSKA, M., GUTAROWSKA, B., BRYCKI, B., 2015. *Multistep approach to control microbial fouling of historic building materials by aerial phototrophs.* Biofouling. 35(3), 284-298.

HAFIDI, Z., GARCÍA, M., Vazquez, S., MARTINAVARRO-MATEOS, M., RAMOS, A., PÉREZ, L., 2025. *Antimicrobial and biofilm-eradicating properties of simple double-chain arginine-based surfactants*. Colloid Surface B. 253, 114762.

JIANG, Y., LIU, L., JIN, B., LIU, Y., LIANG, X., 2024. *Critical review on the environmental behaviors and toxicity of* *triclosan and its removal technologies*. Sci Total Environ. 932, 173013.

ZHANG, J., CHENG, L., LI, H., CHEN, X., ZHANG, L., SHAN, T., WANG, J., CHEN, D., SHEN, J., ZHOU, X., GOU, L., ZHANG, L., ZHOU, X., REN, B., 2025. *Challenges of quaternary ammonium antimicrobial agents: Mechanisms, resistance, persistence and impacts on the microecology*. Sci Total Environ. 958, 178020.

YAO, J., BAN, X., XIE, Y., YIN, W., WANG, Y., XUE, F., 2024. *Research advancement of efficient flotation separation technologies for magnesium-containing minerals*. Green and Smart Mining Engineering. 1(2), 140-156.

HAN, J., LI, X., DAI, S., LIU, G., 2021. *The Flotation Separation of Magnesite and Limonite Using an Amine Collector*. Adsorpt Sci Technol. 2021, 5534274.

LUO, N., SHI, J., YAN, B., WANG, X., 2024. *Flotation Separation of Magnesite from Dolomite Using Sodium Silicate Modified with Zinc Sulfate as a Selective Depressant*. Miner Process Extr M. 14(4), 14040355.

TENG, Q., FENG, Y., LI, H., 2018. *Effects of silicate-bacteria pretreatment on desiliconization of magnesite by reverse flotation*. Colloid Surface A. 544, 60-67.

PAYERL, C., BRAČIČ, M., ZANKEL, A., FISCHER, W., KASCHOWITZ, M., FRÖHLICH, E., KARGL, R., STELZER, F., SPIRK , S., 2017. *Nonspecific protein adsorption on cationically modified Lyocell fibers monitored by zeta potential measurements*. Carbohyd Polym. 164, 49-56.

TIAN, H., WANG, A., CHEN, J., JIANG, X., SHI, J., ZHANG, C., MEI, Y., WANG, B., *Treatment Effect Modeling for FTIR Signals Subject to Multiple Sources of Uncertainties*. Ieee t autom sci eng. 19(2), 895-906.

CHENG, G., MA, Y., LÓPEZ-VALDIVIESO, A., YIN, W., 2024. *Selective depression of phenoxyacetyl chloride on magnesite: Implications for effective flotation separation of magnesite from dolomite*. Miner Eng. 218, 109017.

WANG, E., LI, X., DAI, S., LI, Z., ZHAO, T., SONG, B., HAN, B., 2022. Increased effectiveness of the flotation separation of hornblende and magnesite by adding citric acid as depressant. Tenside Surfact Det. 59(3), 269-279.

LIU, Z., DONG, X., LIAO, Y., FAN, Y., CAO, Y., 2024. *New insights into the adsorption and assembly of mixed collectors with different carbon chain lengths on the low-rank coal flotation by sum-frequency vibration spectroscopy and molecular dynamics simulation*. Powder Technol. 434, 119294.

MOEINI, B., R. LINFORD, M., 2023. *Surface analysis insight note: Initial, statistical evaluation of X-ray photoelectron spectroscopy images*. Surf Interface Anal. 55(8), 572-578.

HU, X., LUO, X., LIU, Z., ZHANG, Y., ZHOU, H., YANG, Z., TANG, X., 2024. *Flotation separation of feldspar from quartz using sodium fluosilicate as a selective depressant*. Rare Metals. 43, 1288–1300.

LIU, W., LIU, W., WEI, D., LI, M., ZHAO, Q., XU, S., 2017. *Synthesis of N,N-Bis(2-hydroxypropyl)laurylamine and its flotation on quartz*. Chem Eng J. 309, 63-69.

YAO, J., SUN, Y., YIN, W., SUN, H., YANG, S., 2025. *Study on the effects of a novel imidazoline siliconophilic collector in the desilication process of magnesite: Separation experiments, adsorption mechanisms, and separation model*. Sep Purif Technol. 353, 128461.

GAO, G., SUN, H., WANG, Y., SUN, Y., HAN, H., YUAN, Z., 2024. *Study on the separation effects of the novel collector ODD on magnesite and quartz*. Physicochem Probl Mi. 60(4), 190522.